Regular Article

ANALYTICAL
AND BIOANALYTICAL
CHEMISTRY
RESEARCH

Published by the
Iranian Chemical Society

***Anal. Bioanal. Chem. Res.**, Vol. 9, No. 2, 141-151, April 2022.*

Feasibility Study of Using graphene Oxide/silica Gel Nanocomposite Prepared by Sol-gel Method for Removing Malachite Green from Aqueous Solutions: Optimization, Kinetic, and Isotherm Studies

Ali Hassanzadeh[a], Ebrahim Ghorbani-Kalhor[a,*], Khalil Farhadi[b] and Jafar Abolhasani[a]

[a]*Department of Chemistry, Tabriz Branch, Islamic Azad University, Tabriz, Iran*

[b]*Department of Analytical Chemistry, Faculty of Chemistry, Urmia University, Urmia, Iran*

(Received 27 May 2021 Accepted 25 October 2021)

The main objective of this work was to evaluate the feasibility of the application of GO/Na_2SiO_3 nanocomposite as a highly efficient adsorbent for the removal of malachite green as a cationic dye from aqueous solutions. To do so, first, the synthesized nanosorbent was characterized *via* FTIR, SEM, TEM and XRD techniques. The surface area and pore mean size of above-mentioned nanocomposite were determined using the BET technique. Also, some important parameters affecting the efficiency of the absorption of malachite green, such as pH, adsorbent dosage, contact time, the primary concentration of dye and salt effect were optimized. The malachite green (water-soluble) dye was analyzed at a maximum wavelength of 618 nm. The optimal conditions for removal of malachite green from aqueous solution included a 20 mg l^{-1} initial concentration with 25 mg adsorbent at pH 7, and adsorption equilibrium was achieved within 5 min. Kinetic studies confirmed that the dye adsorption process followed pseudo-second order kinetic models (R^2 = 0.9999) and adsorption equilibrium data showed a good correlation with Freundlich isotherm (R^2 = 0.9982 at 298 K). Thermodynamic analysis indicates that the adsorption process is spontaneous and exothermic in nature. In addition, the experimental data obtained from reusability studies showed that the prepared adsorbent could be used in up to six adsorption-desorption cycles without a significant decrease in removal efficiency.

Keywords: Graphene, Sodium silicate, Removal, Malachite green, Adsorption isotherm, Kinetic

INTRODUCTION

Along with the progress of different industries such as food, plastics, cosmetics and fabrics, the application of dyes has increased. This vast application field of dyes has made dyes an inseparable part of most wastewaters [1]. In many countries, especially less developed countries, industrial wastewater is discharged into the nearest water resources such as gulfs, lakes, rivers and groundwater reservoirs with no treatment [2]. Generally, dyes are synthetic organic/inorganic compounds with complicated aromatic structures containing different halogen, nitrogen and sulfur-containing functional groups which are very stable and non-degradable [3]. Malachite green, also known as aniline green, victoria green B, basic green 4, and diamond green B, is a cationic organic dye and belongs to triphenyl methane family [4]. Findings have revealed that this dye, especially its reduced form called leucomalachite green, is toxic, carcinogenic, mutagenic and teratogenic. Also, when it is released to the hydrosphere, in addition to creating an unpleasant landscape, it threatens the health of humans and other living kinds [5]. Although the application of this dye is prohibited in many countries, due to its antifungal and antiseptic properties as well as low cost and high water-solubility, it is extensively applied in fish farms to control parasites and fish diseases. Therefore, the removal or decrease of the concentration of this dye in wastewater before discharging to the ecosystem is of critical

*Corresponding author. E-mail: ekalhor@iaut.ac.ir

importance [1,6].

Literature review shows that, along with the failure of physical methods such as oxidation, filtration, chemical degradation, and coagulation in the refinement of active and stable dyes in wastewater [7-10], application of adsorption processes using different adsorbents, especially nano-adsorbents with high capacity, has been highly recommended [11]. In fact, adsorption-based methods not only address limitations such as high cost, complicated processes (multistep processes) and production of high amounts of byproducts [12], but also have higher efficiency, greater diversity, more specificity and reusability [7].

In the past few decades, many nano-adsorbents have been evaluated for the removal, and sometimes pre-concentration, of a variety of organic and inorganic pollutants [11]. Graphene oxide (GO) is a member of carbonaceous materials and has become extensively popular in different research fields due to its high mechanical, thermal and chemical stability. Also, GO contains high amounts of carboxyl, hydroxyl and epoxy groups on its surface making it an ideal candidate with high adsorption capacity for solid-phase extraction and removal processes [13].

However, for these purposes, the application of GO in a composite structure seems to be necessary since it can become irreversibly aggregated (π-π and Van der Waals interactions between planes) resulting in the loss of the efficiency of the structure [14].

Based on the published reports, composite materials made of SiO_2 and GO can address easy coagulation of GO and increase its specific surface area and active site number (for secondary reactions) [15-17]. For example, Mohammadi Nodeh *et al.* applied magnetic GO-silica composite for the removal of naproxen from wastewater. They suggested that analyte adsorption on their prepared adsorbent relied on the π-π interactions between GO and benzene ring of naproxen [18]. Also, Liu et al. reported the application of magnetic hybrid nanocomposites of porous GO-silica for the removal of para-nitrophenol with an adsorption capacity of 1.548 g/g under optimized conditions. Based on their reported characterization, the specific surface area of the nanocomposite structure was 29.3 m^2 g^{-1} and the dominant mechanism of the adsorption process was electrostatic interaction between analyte and nanocomposite [19]. In another work, Wang *et al.* applied tris(indolyl)methane-functionalized silicate-GO composite as adsorbent for the extraction of a variety of organic acids (benzoic acid *p*-methoxybenzoic, salicylic acid, cinnamic acid, *p*-chlorobenzoic acid and *p*-bromobenzoic acid). They reported the specific surface area of their adsorbent to be 135.5 m^2 g^{-1} and claimed that in the presence of tris(indolyl)methane, hydrophilic groups were reduced and amine functional group and π-π interactions were increased resulting in the formation of many hydrogen bonds between analyte and adsorbent [20].

In the present work, we have investigated the application of GO-Na_2SiO_3 nanocomposite synthesized using the sol-gel method for the removal of MG dye from water samples. After the synthesis and characterization of the proposed nanostructures, effective parameters on the adsorption process were optimized according to one at a time protocol. Independently, kinetic and adsorption equilibrium studies were performed and the possible mechanisms of MG adsorption onto as-synthesized adsorbent were debated.

EXPERIMENTAL

Chemicals

All chemicals applied in this research were used as received without further purification. The GO applied was of 99% purity grade and was purchased from Nanosav Company (Tehran, Iran). Na_2SiO_3 (extra pure), methanol (CH_3OH), acetic acid (CH_3COOH), hydrochloric acid (HCl), sodium hydroxide (NaOH) and sodium chloride (NaCl) were obtained from Merck Company (Darmstadt, Germany) and malachite green dye was purchased from St. Louis company (MO, USA). Doubly distilled water obtained from Atlas Company (Iran) was used in all experiments.

Characterization and Spectroscopy

To investigate the functional groups of the synthesized nanocomposite, FTIR spectra were recorded and studied in the wavenumber range of 4000-650 cm^{-1} (Thermo Nicolet instrument, Nexus® 670, USA). Microscopic imaging and the determination of morphology were performed using a scanning electron microscope (SEM) (model: JEOL JEM-

200CX, Japan) and transmission electron microscope (TEM) (model: Karl Zeiss LEO E 906, Germany). X-ray diffraction (XRD) studies were performed on Siemens D5000 device (Germany) equipped with Cu Kα X-ray radiation source (λ = 1.54 Å, 40 KV, 30 Ma). Also, the surface area of the prepared adsorbent was studied using BET technique on a Belsorp II device (Japan) based on the adsorption and desorption isotherms of nitrogen gas at 77 K temperature. All UV-Vis spectroscopy studies in different steps of optimization and measurement were performed using double beam spectrophotometry device PG model GT 80+ (China).

Preparation of GO-Na_2SiO_3 Nanocomposites

In order to prepare GO-silicate composite, which will be denoted as GO/Na_2SiO_3 from now on, the modified method of Choy *et al.* was used [21]. Briefly, GO suspension was prepared by the sonication of a mixture of 20 mg GO in 10 ml deionized water for 2 h. Then, 1 g sodium silicate was added dropwise into the mixture and stirred for further 30 min under an air atmosphere. In the following step, concentrated hydrochloric acid was added dropwise into GO-sodium silica suspension to adjust its pH at 6 (using Zag Shimi pH meter model PTR79, Iran). Once the pH was fixed, stirring was continued for a further 12 h and finally dried on a Teflon plate in the air.

Determination of pH_{pzc}

To determine the pH value of isoelectric point or point of zero charge (pzc), 15 ml deionized water was added into a series of round bottom flasks and their pH values were adjusted using 0.1 M NaOH and HCl to 2, 4, 6, 8, 10 and 12. Then, 25 mg GO/Na_2SiO_3 nanocomposite was added to each solution and the obtained mixture was gently shaken for 24 h. Then, the pH value of adjacent solutions containing nano-adsorbent was measured using a pH meter. Finally, the cross point of the plot of primary pH versus final pH was identified as pH_{pzc} [22].

Batch study and Optimization Procedure

The process of the removal of MG dye from the batch model was also studied. First, a stock solution containing 200 mg l^{-1} dye in distilled water was prepared and used for the preparation of solutions required in the remaining tests. The evaluation of dye concentration in standard and test solutions was performed using a spectrophotometer and drawing calibration curves in the concertation range of 0.5-20 mg l^{-1} and wavelength 618 nm (y = 0.086x-0.0248, R^2 = 0.9989). To determine the behavior of efficient adsorption of MG dye onto proposed adsorbent, the optimization of effective parameters in removal process such as primary dye concentration (1-100 mg l^{-1}), amount of adsorbent (5-50 mg), pH value (2-9), NaCl concentration (1-10 w/v%), contact time (0.15-5 min) and temperature (298-313 K) was performed according to one at a time protocol. In a typical test, a certain amount of GO/Na_2SiO_3 adsorbent was added into a 20 ml dye solution and the obtained mixture was stirred at 150 rpm using a magnetic stirrer at room temperature. After mixing was completed, the mixture was centrifuged at 5000 rpm for 5 min, residual concentrations were measured using calibration curves and the percentage and capacity of adsorption were calculated by Eqs. (1) and (2).

$$\%R = \frac{C_0 - C_e}{C_0} \times 100 \quad (1)$$

$$q_e = (C_0 - C_e) \times \frac{V}{m} \quad (2)$$

where C_0 and C_e (mg l^{-1}) are the primary and residual concentrations of dye, respectively, V (l) is the volume of test solution, m (g) is the weight of adsorbent, R is adsorption percentage and q_e is equilibrium adsorption capacity.

RESULTS AND DISCUSSION

Characterization

In the first step of characterization, microscopic evaluations of the structure and morphology of the synthesized GO/Na_2SiO_3 nanocomposite were performed using SEM and TEM techniques. As presented in the figures, the synthesized nanocomposite had a layered structure (Fig. 1a) and in images with higher magnification (Fig. 1b), it was found that amorphous silica nanoparticles were distributed on the surface of GO. Also, as can be seen in TEM images, GO planes were dark and opaque but silica

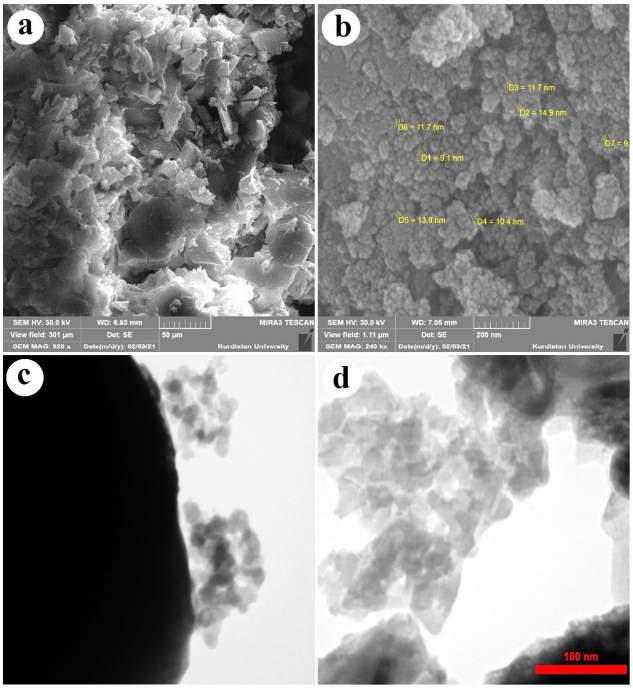

Fig. 1. SEM (a-b) and TEM (c-d) images of GO/Na_2SiO_3 nanocomposite.

nanoparticles were clear and located around GO (Figs. 1c, d). It is noteworthy that, in compliance with many references, silica nanoparticles were located in a chain structure around GO surface and somehow attached GO planes to each other [20].

In this research, FT-IR spectroscopy was used as a reliable and valid technique for the confirmation of the decoration of sodium silicate structure with GO and identification of different groups on the surface of the structure which were responsible for the interaction of analyte and nano-adsorbent. Figure 2a shows the FT-IR spectrum of sodium silicate where a broad band at 3330 cm^{-1} and an intense absorbance bond at 1050 cm^{-1} were observed which could be assigned to symmetric stretching vibrations of O-H bonds in silanol groups on the surface or asymmetric stretching of Si-O-Si, respectively [20]. Also, the band at 795 cm^{-1} could be due to the stretching vibrations of Si-OH [23]. As shown in FT-IR spectrum in Fig. 2b, after decoration with GO, spectral variations observed at 3340 cm^{-1} could be assigned to O-H groups on the surface of GO. Also, the absorbance bond

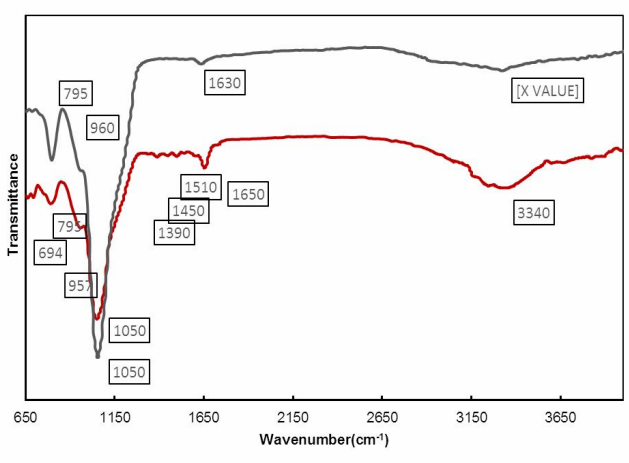

Fig. 2. FTIR spectra of sodium silicate (a) and the synthesized nanocomposite (b).

observed at around 1650 cm^{-1} could be due to carbonyl or carboxyl groups on GO surface which, along with the band at 1390 cm^{-1} (stretching vibration of C-OH) and a weak band at 694 cm^{-1} (bending vibrations of ring C-H), could prove the successful synthesis of GO/Na_2SiO_3 nanocomposite [20].

Figure 3 shows the XRD patterns recorded for sodium silicate and the synthesized nanocomposite. As shown in the figure, the XRD pattern of GO (Fig. 3a) had a relatively sharp 2θ at 10.82°. Also, in the pattern presented for the as-prepared nanocomposite (Fig. 3b), a broad peak was witnessed at 21.36° which showed the dominant effect of silica in the synthesized nanocomposite [24]. A distinct peak at 12.64° verified the presence of GO in the structure [23]. In addition, a weak peak appeared at 34.11° which could be assigned to NaCl [21]. Also, based on Brag law, the d-spacing of the nanocomposite was determined to be 4.13Å.

To study surface area and pore size distribution in the synthesized nanocomposite, N_2 adsorption-desorption isotherms were recorded and investigated (Fig. 4). According to Fig. 4a, N_2 adsorption-desorption isotherms revealed horizontal increase at relatively low pressures ($0 < P/P_0 < 0.3$) which was TYPE 1 according to IUPAC classification and was considered as microporous material [25]. In addition, the results obtained for Brunauer-Emmett-Teller (BET) surface area and pore volume (Fig. 4b)

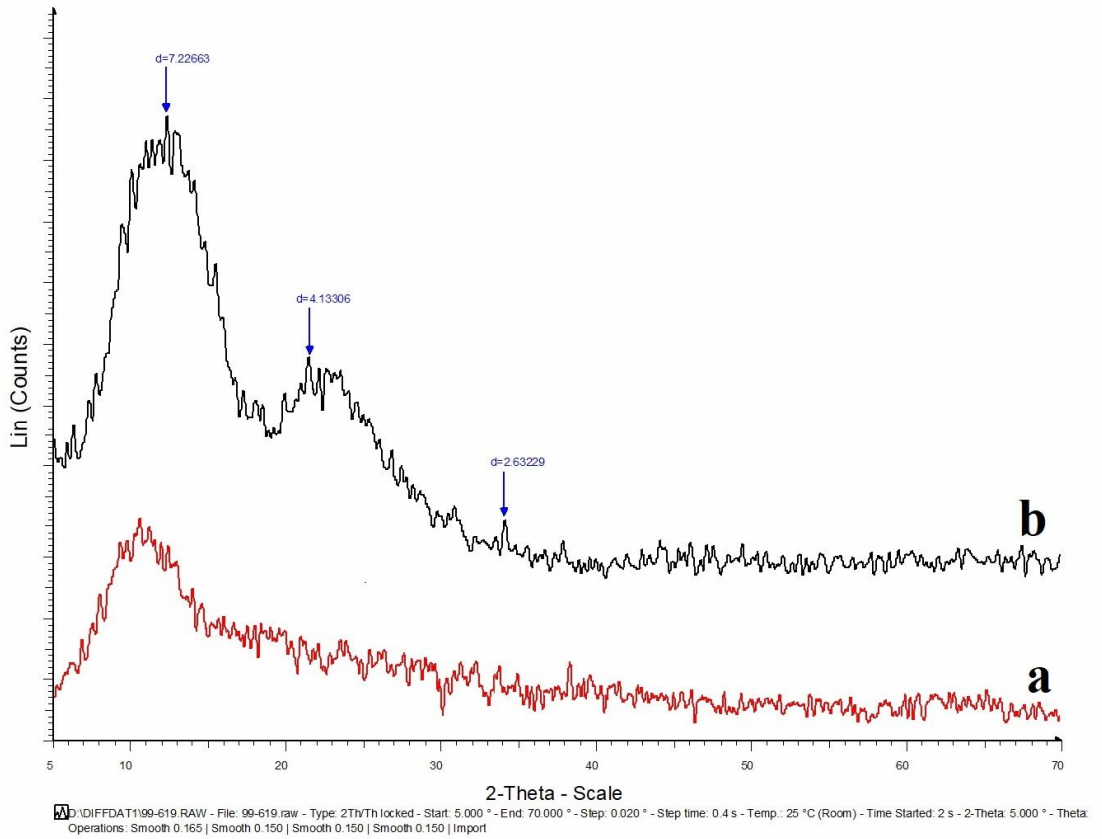

Fig. 3. The XRD patterns of sodium silicate (a), and synthesized nanocomposite (b).

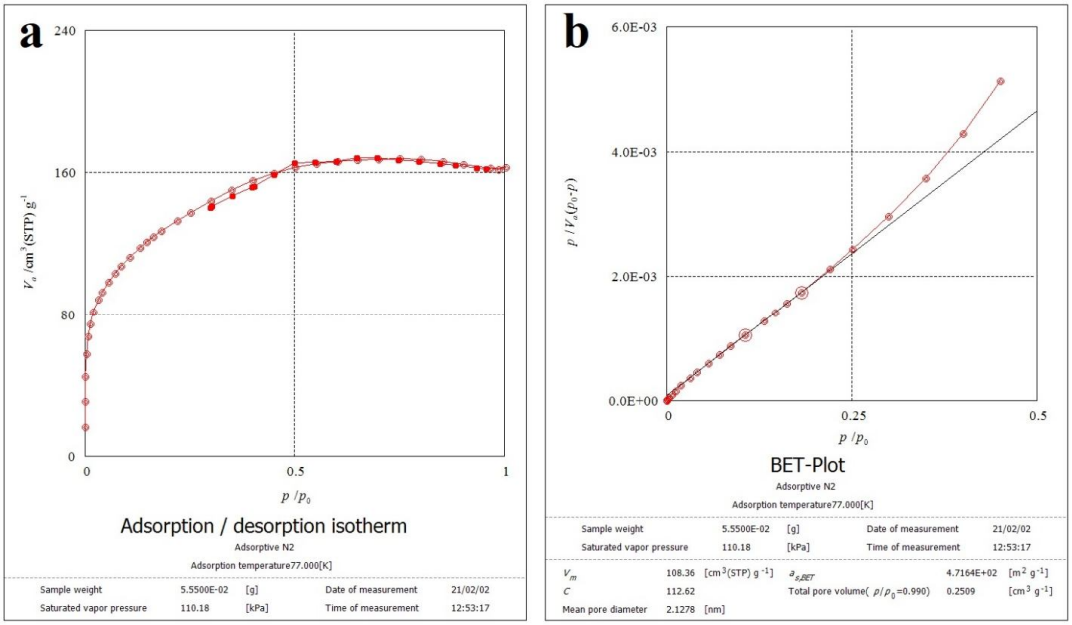

Fig. 4. N_2 adsorption-desorption isotherm (a) and BET-plot (b) of GO/Na_2SiO_3.

confirmed that the prepared nanocomposites had BET surface area of 471 $m^2 g^{-1}$ and pore volume of 0.25 $cm^3 g^{-1}$.

Optimization of the Effective Parameters of Adsorption Process

Primary test and primary dye concentration effect. The amount of dye removal is related to the efficiency of dye adsorbent and primary dye concentration. These parameters were investigated by selecting different concentrations of MG in the range of 1-100 ppm as well as the application of silica-gel (GO-free adsorbent) and adsorbent (25 and 50 mg). The obtained results proved that the undecorated adsorbent could not effectively remove dye while, as expected, the highest removal efficiency of up to 20 ppm was obtained by 25 mg adsorbent (the results are not shown) and at higher concentrations, the amount of adsorption was decreased which could be due to the saturation of adsorbent [26].

pH Effect

As mentioned before, malachite green is a cationic organic dye with the molecular formula $[C_6H_5C(C_6H_4N(CH_3)_2)_2]Cl$ which can exchange hydronium ions on its amine functional groups. Also, it can be applied as a pH change detector in the range of $0.2 < pH < 1.8$. The acidic constant determined for this dye is 10.3. The adsorption peak of MG at wavelength 618 nm was decreased with the increase of pH which indicated the transformation of malachite green to leuco form. In addition, one of the important characteristics of adsorbents in the adsorption process is their pH_{pzc} which indicates the point at which the surface charge of the adsorbent becomes zero (the number of positive and negative charges on the surface become equal). That is to say, at higher pH values than pH_{pzc}, the surface of the adsorbent gets negatively charged and at lower pH values, the surface charge of the adsorbent becomes positive [22]. Hence, considering the role of pH in the variation of the structure and surface charge of analyte and consequently adsorption process, the effectiveness of pH on the removal of MG in the presence of adsorbent in the range of 2-9 was investigated. According to the obtained data (Fig. 5a), the highest efficiency of dye removal using the developed adsorbent was obtained in the pH range of 6-8. In this research, the value of pH_{pzc} for the

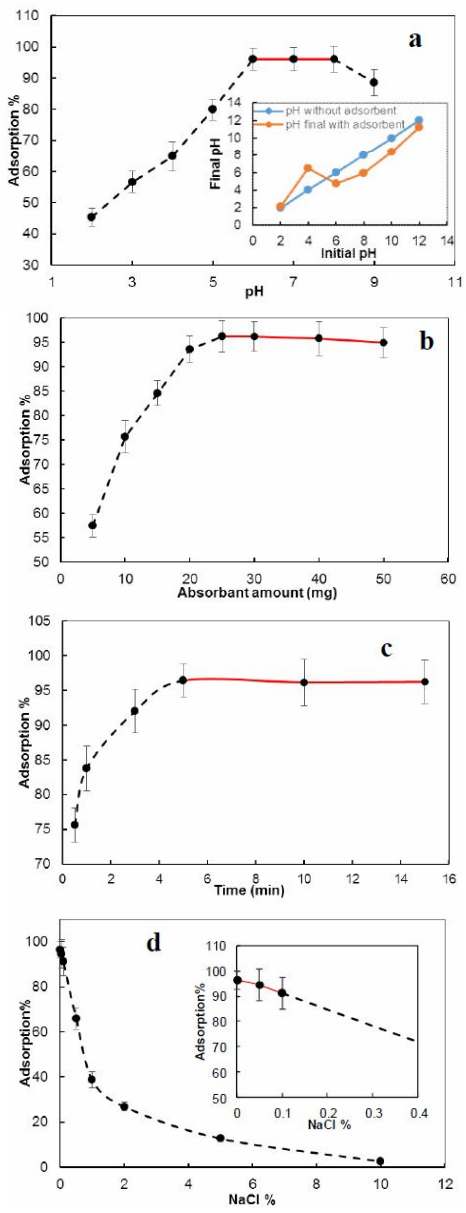

Fig. 5. Optimization of the factors effective in dye removal process, pH effect (the inset shows the determined pH_{pzc} for the adsorbent) (C_{MG}: 20 mg l^{-1}, V: 20 ml, adsorbent amount: 25 mg, contact time: 10 min) (a), adsorbent amount effect (C_{MG}: 20 mg l^{-1}, V: 20 ml, pH: 7, contact time: 10 min) (b), contact duration (C_{MG}: 20 mg l^{-1}, V: 20 ml, pH: 7, adsorbent amount: 25 mg) (c), and NaCl effect (C_{MG}: 20 mg l^{-1}, V: 20 ml, pH: 7, adsorbent amount: 25 mg, contact time: 5 min) (d) (the inset shows the range of salt concentration to be 0.5-2%).

adsorbent was determined to be 5.3 (the inset of Fig. 5a) and since MG is a cationic dye, decrease of its adsorption at pH values of below 5.3 could be due to the positive surface charge of the adsorbent and electrostatic repulsive forces between dye and adsorbent. In pH values of higher than 5.3, the surface charge of adsorbent becomes negative and therefore, due to electrostatic attraction between adsorbent and dye, adsorption efficiency and capacity were increased [22]. Also, according to the claim made by Muinde *et al*., the decrease observed at pH values higher than 8 could be due to the formation of soluble hydroxyl complexes [27].

Adsorbent Concentration Effect

In this research, the effect of adsorbent concentration was evaluated using different amounts of adsorbent in the range of 5-50 mg and the obtained results are shown in Fig. 5b. According to the figure, an increase in the amount of adsorbent from 5 to 15 mg increased dye removal percentage from 57.4 to 84.6% and further increase of adsorbent dose to 25 and 40 mg increased dye removal percentage to 96.2 and 95.8%, respectively. Finally, using 50 mg adsorbent resulted in a slight decrease in dye removal efficiency. Since nano-adsorbents have very high surface-to-volume ratios, the increase of contact surface and the active surface provides higher access to adsorption sites which can result in more effective adsorption, even at lower concentrations of adsorbent [1]. Also, according to the study performed by Guechi and Hamdaoui, relative stability followed by a slight decrease in removal despite the increase of the amount of adsorbent could have two reasons: split in flux or concentration slope between the concentration of minerals in the solution and that at the adsorbent surface and the overlap of adsorption sites on the surface [28]. However, following the study of the adsorbent amount effect, increasing the adsorbent to 50 mg shows an almost constant efficiency of dye removal, therefore, 25 mg of prepared nano-adsorbent was considered as an optimal amount for further experiments.

Contact Time

Mass transfer and equilibrium of the distribution of target species between solution bulk and adsorbent surface as well as analyte diffusion to inner layers of adsorbent are time-dependent phenomena [29]. In fact, at primary contact times, analyte diffusion on the adsorbent surface had the most important effect on adsorption efficiency and as time passed, along with the penetration of analyte to inner adsorption sites, the rate of the adsorption process was decreased [30]. Therefore, in the present study, the effect of contact duration on the efficiency of removal in the time range of 1-15 min was investigated while other parameters were kept constant; the obtained results are shown in Fig. 5c. As was seen, the equilibrium time required for the maximum efficiency of the developed adsorbent was 5 min after which the removal amount was remained almost constant with no significant variation, therefore, this time was chosen as the optimal time.

Salt Effect

Figure 5d shows the salt effect (ionic strength) on the amount of adsorbed dye onto the developed nano-adsorbent. For this objective, a series of dye solutions with different NaCl concentrations in the range of 0-10 wt.% were prepared and their adsorptions were studied under optimal conditions. It was found that the increase of NaCl concentration significantly decreased adsorption efficiency. This behavior could be due to the competition between the analyte and Na^+ ion to reach active adsorption sites. In addition, at high salt concentrations, electrostatic interactions between adsorbent and analyte as well as dye activity coefficient were also affected resulting in the decrease of the efficiency of the developed process [28]. Another claim is that the increase of the ionic strength of the environment could increase the coagulation of dye molecules which could decrease their solubility and adsorption process [31]. Therefore, these results confirm that in the lower the ionic strength of the sample solution (based on the intended experimental model, $C_{NaOH} < 0.1\%$), the proposed adsorbent efficiency will be higher than 90%.

Kinetic and Isotherm Studies

Adsorption consists of a series of mass transfer steps and is generally defined as the accumulation of samples onto the surface of a liquid or solid material (adsorbent). The data of adsorption isotherm is one of the most important data in designing adsorption systems [32]. These mathematical patterns describe the interaction method between adsorbent and adsorbed mass and the relative

distribution of analyte molecules between solution and adsorbent at a certain temperature under equilibrium conditions. Therefore, these studies paved the way to determine the mechanism, surface characteristics, adsorbent tendencies, capacity, and optimization of adsorbent application [33]. Experimental data could be correctly investigated using multiple isotherm models to find the most suitable model for designing the process. In this work, a linear form of Langmuir and Freundlich isotherms for the adsorption of MG by GO/Na_2SiO_3 nanocomposite was studied.

Langmuir Model

As known, this model investigates the adsorption of analyte as a monolayer by assuming a uniform distribution of active adsorption sites and eliminating the counter-effects of the adsorbed molecules [32]. In fact, the key assumption in this model is that intermolecular forces are sharply decreased with the increase of distance and therefore, the prediction of the presence of a monolayer of analyte on the outer surface of the adsorbent was realized [34]. The linear form of Langmuir model is described using Eq. (3) which could ideally estimate q_{max}.

$$\frac{C_e}{q_e} = \frac{1}{K_{q_{max}}} + \frac{C_e}{q_{max}} \quad (3)$$

where C_e (mg l^{-1}) is equilibrium concentration, q_e (mg g^{-1}) is adsorption capacity at equilibrium, q_{max} (mg g^{-1}) is maximum adsorption capacity and K is Langmuir coefficient. q_{max} and K are calculated based on the slope and intercept of linear curve of C_e/q_e *vs*. C_e. Fig. 6a shows Langmuir isotherm model of dye adsorption process using the developed adsorbent at four temperatures of 298, 303, 308 and 313 K and Table 1 summarizes the calculated values of q_{max}, K and R^2 for the above-mentioned model at these temperatures.

Freundlich Model

Freundlich isotherm, as an experimental and empirical model, evaluates the molecular adsorption process of analyte as a multistep phenomenon assuming non-uniform distribution of adsorption sites on the surface or the presence of various sites with various affinities [30].

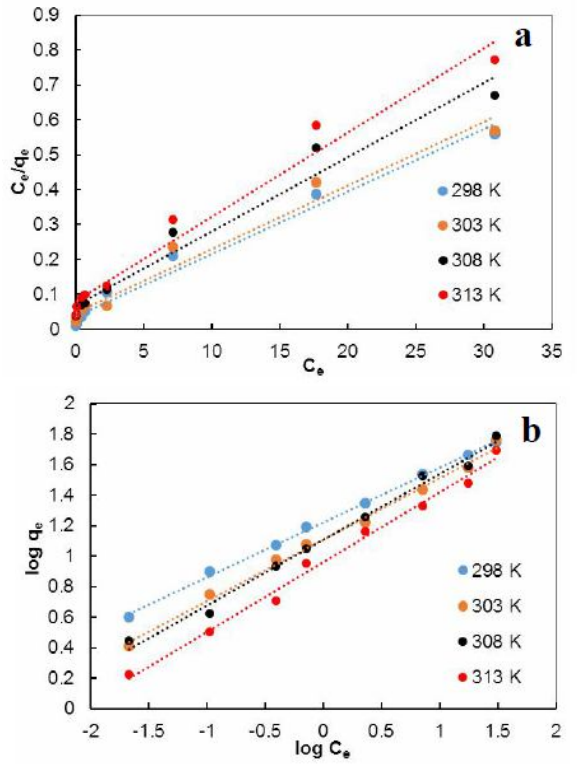

Fig. 6. Adsorption isotherms of Langmuir (a) and Freundlich (b) models (C_{MG}: 5-100 mg l^{-1}, V: 20 ml, pH: 7, adsorbent amount: 25 mg, contact time: 5 min).

Table 1. The Calculated Values of q_{max}, K and R^2 for Langmuir Model at Different Temperatures

Langmuir	298 K	303 K	308 K	313 K
q_{max} (mg g^{-1})	56.17978	54.94505	46.94836	41.49378
R^2	0.9782	0.9702	0.9952	0.9881
K	0.370833	0.379167	0.318386	0.296069

Equation (4) shows the linear form.

$$\log q_e = \frac{1}{n}\log C_e + \log k_f \quad (4)$$

where C_e (mg l^{-1}) and q_e (mg g^{-1}) are equilibrium concentration and adsorption capacity under equilibrium

conditions, respectively, and k_f and n are Freundlich isotherm constants such that k_f is considered as a factor related to bond energy and shows the amount of analyte adsorbed onto the adsorbent. Also, n determines the degree of nonlinearity between the concentration of dye and adsorbent such that if n = 1, the adsorption is linear. However, when n < 1, the adsorption process is chemical and when n > 1, the mechanism of the adsorption process is physical [35].

Using the curve of $\log q_e$ *vs.* $\log C_e$, the values of n and k_f could be obtained from the slope and intercept of the plot, respectively, which were calculated at four temperatures of 298, 303, 308 and 313 K, as presented in Table 2 and

Investigation of adsorption isotherms at four temperatures showed that, among the isotherms, equilibrium data obtained from Freundlich isotherms with regression coefficient 0.9982 were better than those obtained from Langmuir isotherm with regression coefficient 0.9782 at 298 K. Therefore, these results could prove the non-homogenous process of dye adsorption onto an adsorbent while adsorbent molecules interacted with each other as Fig. 6b.

well (analyte molecule adsorption as multilayer). In addition, since the value of n parameter was calculated to be 2.8 (n > 1), the physical adsorption of MG onto the developed adsorbent was verified [32].

Kinetic Studies

Dye adsorption rate depended on time because dye molecules should first face with border effect, then be adsorbed from solution bulk, and finally penetrate into adsorbent core [30]. Kinetic models can also provide information on adsorption paths and their probable mechanisms and are therefore critical for developing the process and design of adsorption systems. To fit experiment data for adsorption kinetics identification, several models including pseudo-first-order, pseudo-second-order, second-order, and intra-particle diffusion models were investigated.

In this work, the kinetic constants of adsorption were calculated according to related equations (Eqs. (5)-(8)) and the best theoretical model was selected based on the comparison of the linear regression determination coefficients (R^2) values.

Table 2. The Values of n, k and R^2 calculated for Freulndlich Isotherm Model

Freundlich	298 K	303 K	308 K	313 K
n	2.798769	2.483855	2.327205	2.19106
k_f	13.24555	12.90031	12.83808	9.126411
R^2	0.9982	0.9939	0.9911	0.9914

$$\log(q_e - q_t) = \log q_e - \left[\frac{k_1}{2.303}\right]t \quad (5)$$

pseudo-first-order

$$t/q_t = (1/k_2\, q_e^2) + t/q_e \quad (6)$$

pseudo-second-order

$$1/(q_e - q_t) = 1/q_e + k_t\, t \quad (7)$$

Second-order

$$q_t = k_{id}\, t^{0.5} + C \quad (8)$$

intra-particle diffusion

where qe and q_t (mg g^{-1}) are the amounts of adsorbed MG at equilibrium and other times in terms of minutes, respectively. Also, k_1 (min^{-1}), k_2 (g mg^{-1} min^{-1}), k_{id} (mg g^{-1} $min^{-0.5}$) and k_t are the rate constants of pseudo-first-order, pseudo-second-order, second-order and intra-particle diffusion states, respectively. In the pseudo-first-order kinetic model, the adsorption rate depended on the empty sites on the surface of the adsorbent while in the pseudo-second-order kinetic model, the adsorption rate was proportional to the square of the empty sites. Intra-particle penetration is a penetration-based model which is used to describe multistep adsorptions (generally including the transfer of dye molecules from aqueous phase onto adsorbent surface followed by their penetration into the internal space of solid particles) where competitive adsorption takes place [30,36]. Fitting curves of kinetic models along with experimental curves are shown in Fig. S1. The obtained results showed that the pseudo-

Table 3. The Values of q_e, k and R^2 for Different Kinetic Models

Order	q_e (mg g^{-1})	k	R^2
Pseudo 1st	2.588	0.3408 min^{-1}	0.9384
Pseudo 2nd	15.5763	0.4793 g mg^{-1} min^{-1}	0.9999
2nd order	0.3582	2.6598 g mg^{-1} min^{-1}	0.9803
Intra-particle diffusion	12.408	0.9421 mg g^{-1} $min^{0.5}$	0.7143

second-order kinetic model presented the best fitting and it was found that the chemical absorption step was the limiting step. Detailed information on rate constant values for different studied models is provided in Table 3.

In addition, the data obtained from the isotherms of adsorption processes and kinetic studies as well as those obtained for pH effect and the correlation of pH_{pzc} results proved that electrostatic interactions could be the main mechanism in the adsorption process of MG using GO/Na_2SiO_3, although based on FT-IR characterization, interactions such as hydrogen bonding and π-π stacking could also be involved [37]. To investigate of the temperature effects on the adsorption of malachite green dye using as-prepared nanocomposite, thermodynamic equilibrium coefficients at different temperatures were calculated and inserted in Supporting Information. Also, compares q_{max} (mg g^{-1}), isotherm, kinetics, and thermodynamic study of some adsorbents that were previously employed for the removal of MG from aqueous solution were given in Table S3.

Desorption and Reusing of the Adsorption

In order to address economic, environmental and practical application concerns of the developed adsorbent, its reusability was also evaluated. For this purpose, the adsorbent was used for six consecutive adsorption-desorption cycles (under optimal conditions). It is noteworthy that, between every two cycles, the desorption and cleaning of the surface of the adsorbent were performed using 2 ml mixture solution of 95% (v/v) methanol and 5% (v/v) acetic acid under vortex (2 min) [38] followed by repeating the same procedure with distilled water for two cycles.

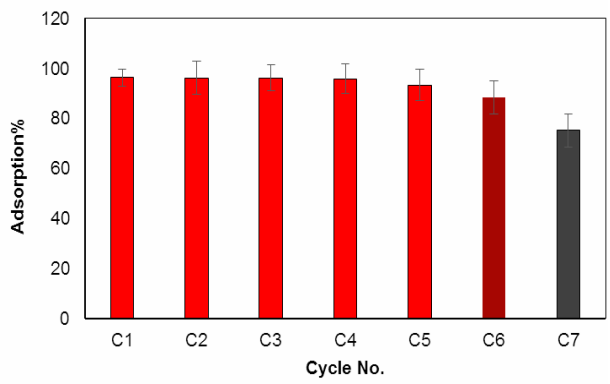

Fig. 7. Adsorption-desorption cycles for the evaluation of the reusability of the adsorbent (C_{MG}: 20 mg l^{-1}, V: 20 ml, pH: 7, adsorbent amount: 25 mg, contact time: 5 min).

As shown in Fig. 7, the obtained results showed that there was no significant decrease in the amount of MG adsorption up to the 5th cycle (STDEV = 1.29) while in the 6th cycle, the removal efficiency was decreased significantly and in the 7th cycle, less than 80% of the efficiency of the first 5 cycles was obtained. This finding verified the practical application of the developed adsorbent as a low-cost, facile and reusable adsorbent.

CONCLUSIONS

Batch adsorption research showed that the removal of MG using GO/Na_2SiO_3 nanocomposite was successfully performed. The obtained results showed that 25 mg developed adsorbent in 20 ml sample (20 ppm) at ambient temperature in neutral pH range in contact duration of 5 min could remove more than 95% of the dye. The q_{max} values of the adsorption of MG dye on the proposed adsorbent were 56.18 mg g^{-1} at room temperature. Adsorption equilibrium was in good agreement with Freundlich adsorption isotherm which proved the adsorption of analyte molecules in a multilayer manner on the non-homogenous surface of the adsorbent and based on the obtained constants, the physical adsorption of the analyte was proved.

Also, based on the performed calculations, among the four conventional kinetic models, pseudo-second-order

kinetic model provided the highest fitting. The values of thermodynamic parameters such as a change in Gibbs free energy, enthalpy, and entropy revealed the exothermic and spontaneous nature of the adsorption process. Reusability studies showed that the adsorbent was capable of being used in at least 6 adsorption-desorption cycles preserving at least 92% of its primary efficiency.

REFERENCES

[1] M. Amiri, M. Salavati-Niasari, A. Akbari, T. Gholami, Int. J. Hydrogen Energ. 42 (2017) 24846.

[2] Y.D. Liang, Y.J. He, Y.H. Zhang, Q.Q. Zhu, J. Environ. Chem. Eng. 6 (2018) 416.

[3] G. Absalan, A. Bananejad, M. Ghaemi, Anal. Bioanal. Chem. Res. 4 (2017) 65.

[4] K. Tewari, G. Singhal, R.K. Arya, Rev. Chem. Eng. 34 (2018) 427.

[5] N.E. Sabiha, S. Rahman, Sustainability 10 (2018) 1580.

[6] G. Sriram, U.T. Uthappa, M. Kigga, H.Y. Jung, T. Altalhi, V. Brahmkhatri, M.D. Kurkuri, New J. Chem. 43 (2019) 3810.

[7] L. Adlnasab, M. Shabanian, M. Ezoddin, A. Maghsodi, Mater. Sci. Eng. B 226 (2017) 188.

[8] C.K.C. Araújo, G.R. Oliveira, N.S. Fernandes, C.L.P. S. Zanta, S.S.L. Castro, D.R. Da Silva, C.A. Martínez-Huitle, Environ. Sci. Pollut. Res. 21 (2014) 9777.

[9] S. Mondal, Environ. Eng. Sci. 25 (2008) 383.

[10] H.S. Rai, M.S. Bhattacharyya, J. Singh, T.K. Bansal, P. Vats, U.C. Banerjee, Crit. Rev. Env. Sci. Technol. 35 (2005) 219.

[11] M. Ghaedi, N. Mosallanejad, J. Ind. Eng. Chem. 20 (2014) 1085.

[12] M. Abbasi, J. Clean. Prod. 145 (2017) 105.

[13] S. Yang, D. Zhang, H. Cheng, Y. Wang, J. Liu, Anal. Chim. Acta 1074 (2019) 54.

[14] M. Ma, H. Li, Y. Xiong, F. Dong, Mater. Des. 198 (2021) 109367.

[15] Y. Cao, X. Li, Adsorption 20 (2014) 713.

[16] S. Mahpishanian, H. Sereshti, M. Ahmadvand, J. Environ. Sci. 55 (2017) 164.

[17] R. Alam, M. Mobin, J. Aslam, Surf. Coat. Technol. 307 (2016) 382.

[18] M.K. Mohammadi Nodeh, M. Radfard, L.A. Zardari, H. Rashidi Nodeh, Sep. Sci. Technol. 53 (2018) 2476.

[19] F. Liu, Z. Wu, D. Wang, J. Yu, X. Jiang, X. Chen, Colloids Surf., A 490 (2016) 207.

[20] N. Wang, H. Yu, S. Shao, J. Sep. Sci. 39 (2016) 1700.

[21] J.S. Choi, H.K. Lee, S.J. An, RSC Adv. 5 (2015) 38742.

[22] T.P. Krishna Murthy, B.S. Gowrishankar, M.N. Chandra Prabha, M. Kruthi, R. Hari Krishna, Microchem. J. 146 (2019) 192.

[23] W.L. Zhang, H.J. Choi, Langmuir 28 (2012) 7055.

[24] X. Guo, X. Liu, B. Xu, T. Dou, Colloids Surf., A 345 (2009) 141.

[25] Z.A. Alothman, Materials 5 (2012) 2874.

[26] T.H. Liou, M.H. Lin, Sep. Sci. Technol. 55 (2020) 431.

[27] V. M. Muinde, J. M. Onyari, B. Wamalwa, J. Wabomba, R. M. Nthumbi, J. Environ. Prot. 8 (2017) 215.

[28] E.K. Guechi, O. Hamdaoui, Arab. J. Chem. 9 (2016) S416.

[29] A.A. Asgharinezhad, H. Ebrahimzadeh, F. Mirbabaei, N. Mollazadeh, N. Shekari, Anal. Chim. Acta 844 (2014) 80.

[30] J. Mohanta, B. Dey, S. Dey, ACS Omega 5 (2020) 16510.

[31] D. Karadag, E. Akgul, S. Tok, F. Erturk, M.A. Kaya, M. Turan, J. Chem. Eng. Data 52 (2007) 2436.

[32] E. Boorboor Azimi, A. Badiei, J.B. Ghasemi, Appl. Surf. Sci. 469 (2019) 236.

[33] E.A. Abdelrahman, J. Mol. Liq. 253 (2018) 72.

[34] M.A. Ahmad, N. Ahmad, O.S. Bello, J. Disper. Sci. Technol. 36 (2015) 670.

[35] G. Crini, H.N. Peindy, F. Gimbert, C. Robert, Sep. Purif. Technol. 53 (2007) 97.

[36] Y. Guo, Y. Mo, M. Wang, H. Cui, Y. Tang, T. Sun, J. Mol. Liq. 329 (2021) 115529.

[37] R. Ben Arfi, S. Karoui, K. Mougin, C. Vaulot, L. Josien, G. Schrodj, L. Michelin, A. Ghorbal, Int. J. Environ. Anal. Chem., DOI: 10.1080/ 03067319.2020.1828389(2020) 1.

[38] S. Banerjee, G. Sharma, R. Gautam, M. Chattopadhyaya, S.N. Upadhyay, Y.C. Sharma, J. Mol. Liq. 213 (2016) 162.